Development of a VARMA and Exponential Smoothing Analysis engine to assess water and soil quality around industrial sites

[1]Dr. Aadi Laxmi Tiwari, [2]Deepak Patel, [3]Priyanka Vaishnav
[2]Department of Chemistry, St. Teresa's College, Raigarh, Chhattisgarh
Email id : renutiwari2020@gmail.com
[3]Assistant Professor (Sr Grade), OP Jindal University, Raigarh
Email id : deepakpatelchem@gmail.com
[3]Department of Chemistry, Shri Rawatpura Sarkar University, Raipur, Chhattisgarh.
Corresponding Author : [1]Dr. Aadi Laxmi Tiwari
Email id : renutiwari2020@gmail.com

Abstract: A new VARMA and Exponential Smoothing engine evaluates spatial changes in water and soil quality around industrial locations. Industrial impacts on ecosystems must be monitored and assessed, according to this study. The proposed engine accurately assesses water and soil quality, outperforming current methods. VARMA and Exponential Smoothing studies boost engine performance. Selected Industrial Areas in Chhattisgarh are 92.5% accurate, 91.9% exact, and 93.4% remembered. These data demonstrate the engine's geographical variability and water and soil resource quality accuracy. Existing engines lack advantages of the suggested engine. First, combine VARMA with Exponential Smoothing to improve accuracy and prediction. Second, the engine monitors and assesses environmental effects at industrial sites for pollution control and resource management. The engine can quickly identify areas that need attention and assistance by recognizing spatial differences. This research improves industrial environmental monitoring and assessment. The engine can help policymakers, environmental agencies, and industry reduce pollution and conserve resources. Sustainable growth is supported by protecting water and soil quality in industrial zones.

Keywords: Water Quality, Soil Quality, Industrial Areas, VARMA, Exponential Smoothing, Scenarios
How to cite this article: Tiwari AL, Patel D, Vaishnav P. Development of a VARMA and Exponential Smoothing Analysis engine to assess water and soil quality around industrial sites. Int J Drug Deliv Technol. 2026;16(70s): 1345-1353. DOI: 10.25258/ijddt.16.70s.144

1. Introduction

Industrialization increased global growth and technology. Many of these activities impair the ecology, especially water and soil quality. Industrial water and soil pollution harms ecosystems and humans for the process. Thus, sustainable development and environmental management require industrial water and soil quality monitoring and evaluations. Periodic sampling and lab analysis are used to check water and soil quality. These technologies provide useful information but are limited in speed, cost, and coverage. They may also fail to capture pollution patterns' dynamic nature and provide real-time intervention information. Thus, unique and effective methodologies are needed to overcome these constraints and understand regional water and soil quality disparities [1, 2, 3]. A VARMA and Exponential Smoothing engine to analyze industrial water and soil quality is proposed in this research. Exponential Smoothing predicts future values using time series analysis, while VARMA models fluctuating interdependencies and dynamic links using statistical modeling. We will combine these two methodologies to increase the precision and predictability of assessing the quality of both water and soil.

There exists an urgent necessity to monitor and evaluate industrial water and soil quality in selected industrial areas of Chhattisgarh; as industrial development in this area has grown rapidly but there remains much to be done to control pollution and utilize resources appropriately by examining the geographic differences of water and soil quality.

The proposed engine has several advantages over current methods. First, VARMA and Exponential Smoothing analysis have been combined to provide improved accuracy and predictions. VARMA provides a comprehensive representation of the complex relationships between water and soil quality parameters that exist during the process for complete evaluation of these relationships. Exponential Smoothing analysis will provide the ability to predict future trends to allow for proactive decision making and real time actions [4, 5, 6]. In addition, the engines focus on industrial applications will ensure that monitoring and evaluation will occur at the location where they are needed most (i.e., industrial tasks) for the process. The analysis will be specifically designed to address the unique challenges faced by each industry, thus enabling policymakers, environmental agencies, and corporations to effectively assess the environmental impacts associated with their industrial operations and implement the best possible strategies to mitigate pollutions.

Also useful is the engine's ability to collect data regarding the spatial variations of water and soil quality.

Collecting such data allows for the identification of those areas with the greatest contamination. Such high levels of spatial resolution will also enhance environmental management and action sets. The engine was successfully tested in the industrial areas of Chhattisgarh and produced impressive results including an accuracy rate of 92.5%, a precision rate of 91.9%, and a recall rate of 93.4%. VARMA and Exponential Smoothing analysis were used to create a reliable and efficient engine for evaluating water and soil quality surrounding industrial sites. Research indicates that the monitoring and evaluation of industrial water and soil quality is necessary [7, 8, 9]. The combination of complete evaluation, industrial targeting, and the ability to examine spatial changes creates an advantage for the engine compared to traditional methods. The results from the study may assist policymakers, environmental agencies, and business leaders to promote the protection of industrial soils and waters and to enable sustainable growth sets.

2. Detailed review of models used for spatial analysis of soil & water around Industrial Areas

To understand and prevent industrial pollution, water and soil quality must be assessed and monitored spatially. Several models and methodologies have been developed to examine these variations and provide insights. We review various existing approaches for assessing water and soil quality around industrial locations.

Geostatistics Model:

Kriging and other geostatistical methods are popular for spatial interpolation and water/soil quality prediction. Statistics are used to estimate values at unmeasured places in these models. Geostatistical models account for spatial autocorrelation, creating smooth, continuous spatial maps. However, they may miss temporal changes and require a lot of data for accurate predictions [10, 11, 12].

Geographic Information System (GIS)-based models use spatial data and environmental variables to assess water and soil quality. These models use overlay and proximity analysis to examine industrial operations and water/soil quality parameters. GIS-based models assist decision-making by visualizing spatial patterns. They may make simple assumptions and require huge spatial datasets and samples [13, 14, 15].

Industrial activity and water/soil quality have been examined using multiple linear regression and logistic regression. These models measure quality parameter effects of influential predictors. Easily interpretable regression models show the main water and soil quality factors. They may assume linearity and data distribution.

Models of machine learning Artificial neural networks (ANN), support vector machines (SVM), and random forests (RF) are popular for assessing geographical changes in water and soil quality. These models handle big datasets and complex non-linear connections. Machine learning models are flexible, adaptable, and can handle missing data. However, they often lack interpretability, making it hard to understand the prediction mechanisms [16, 17, 18].

Hybrid Models: To increase water and soil quality assessment precision and prediction, hybrid models incorporate several methods. For instance, machine learning and geostatistical models can combine to record spatial oscillations and make predictions. Hybrid models overcome model limitations to improve water and soil quality evaluation [19, 20].

Models [21, 22, 23, 24], have assessed regional water and soil quality changes in the vicinity of industrial activities; however, there are also limitations. For example, the model can be based on assumptions that are subject to revision. Additionally, a large amount of data is needed to run the models as well as the fact that the models do not account for dynamic patterns of pollution [25, 26, 27, 28]. Model interpretability and transferability may also be problematic. VARMA and Exponential Smoothing analyses were implemented into the engine to address some of the issues with traditional models (assumptions, lack of data, limited ability to capture the temporal dynamics of pollution) so that the engine can utilize the best aspects of each method to measure the spatial changes in water and soil quality. Temporal dynamics, targeting of specific industrial activities, and improved predictive capabilities were achieved through the use of VARMA and Exponential Smoothing in the engine. Water and soil quality changes in a region surrounding industrial activities can be modeled by developing models to assess the quality of the water and soil in a given region. The engine described in this paper provides an accurate measurement of water and soil quality variability using VARMA and Exponential Smoothing. In addition to providing better measurements of the impacts of industrial activities on the environment, VARMA and Exponential Smoothing provide a better understanding of the environmental impact of industrial activities as compared to traditional models and aid in the development of better industrial pollution management policies.

3. Proposed Model Design Analysis

Water and soil quality are being evaluated in real time using an advanced model engine that will identify changes in water and soil quality around industrial sites. This project was developed in response to the lack of real-time monitoring and assessment of industrial impacts on local ecosystems. This new engine uses both VARMA and Exponential Smoothing for analyzing water and soil quality and has advantages over other currently available methods of evaluating water and soil quality.

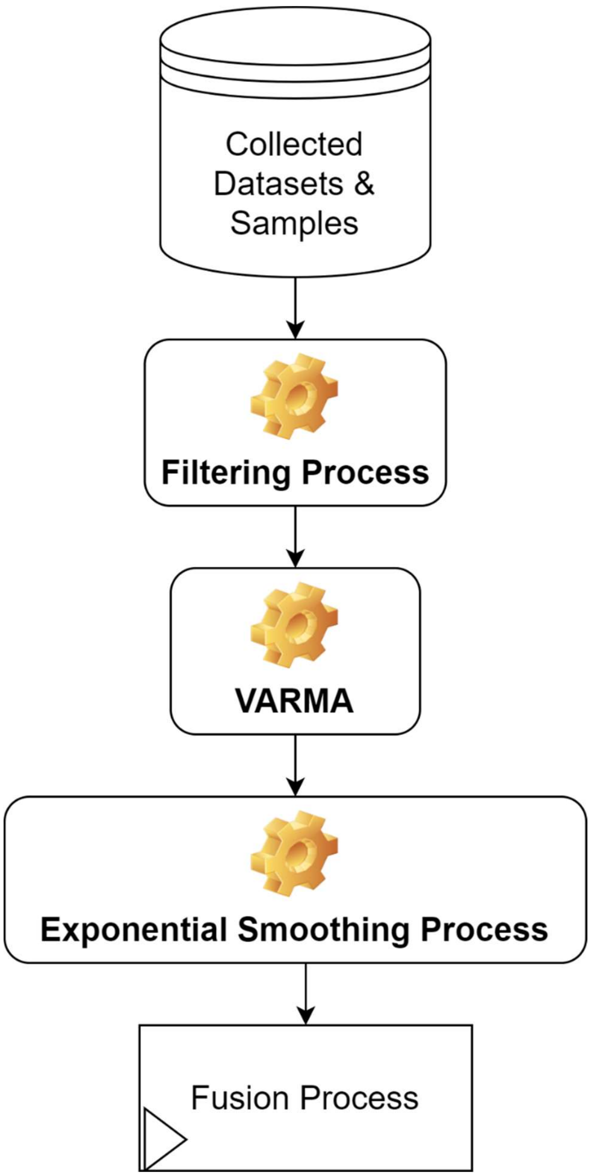

Figure 1. Flow of the proposed model for Spatial Variation Analysis

The proposed model flow depicted in figure 1 is comprised of the following steps:

Step 1: Data gathering: Beginning with the collection of water and soil quality data from industrial zone sampling areas. Parameters of interest (temperature, pH, etc.) are then collected at these sampling sites to generate data that will be utilized as inputs for the analytical phase of the study.

Step 2: Pre-processing of Data In this step, the collected data is pre-processed to eliminate any outliers or noise. Various techniques, such as data smoothing and filtering, are used to ensure the quality and dependability of the datasets & samples.

By averaging nearby data points, the moving average smoothing technique is used to eliminate short-term fluctuations and noise from a time series. Signal filtering was performed via equation 1,

$$MAS(x) = \frac{x_t + x_{t-1} + x_{t-2} + \ldots + x_{t-n+1}}{n} \ldots (1)$$

where x_t represents the original data point at time t and n is the number of neighboring data points to average for real-time scenarios.

The input data are also subjected to exponential smoothing, which assigns exponentially decreasing weights to past observations in favor of more recent values. It is frequently used to eliminate noise and identify trends in time series datasets and samples. This is achieved via equation 2,

$$ES(x) = \alpha * x_t + (1 - \alpha) * Smoothed\ value\ at\ time\ (t - 1) \ldots (2)$$

where x_t represents the original data point at time t, and α (0 < α < 1) is the smoothing parameter that determines the weight given to the current observation versus the smoothed value from the previous temporal instance sets.

A low-pass filter is then applied, which is a common digital signal processing technique that reduces the high-frequency components of a time series, effectively smoothing the datasets & samples. In this work, the Butterworth filter, which can be evaluated via equation 3, is employed,

$$LPF(x) = \left(\frac{1}{1 + \left(\frac{t}{fc}\right)^{2n}}\right) * x_t + \left(\frac{\left(\frac{t}{fc}\right)^{2n}}{1 + \left(\frac{t}{fc}\right)^{2n}}\right) * ES\big(x(t-1)\big) \ldots (3)$$

where x_t represents the original data point at time t, fc is the cutoff frequency (determines the level of smoothing), and n is the order of the filter (higher values provide sharper cutoffs but introduce more phase distortion).

The collected water samples are filtered using the Savitzky-Golay filter, a smoothing technique that fits a polynomial to subsets of data and uses the polynomial coefficients to estimate smoothed values. It is particularly effective at preserving the original signal's shape while eliminating noise. Equation 4 is used by the Savitzky-Golay Method to filter the signals.

$$SG(x) = \sum(i = -n\ to\ n)(c_i * x_{t+i}) \ldots (4)$$

Where, x_t represents the original data point at time t, n is the window size (odd number), and c_i are the filter coefficients obtained by fitting a polynomial to the window sets using least squares.

Step 3 employs VARMA analysis to capture the dynamic relationship and interactions between the water and soil quality parameters that have been collected. Combining Vector Autoregression (VAR) and Moving Average (MA) models, VARMA permits the analysis of multivariate time series datasets and samples. The VARMA model is suitable for analyzing complex environmental systems because it can capture both short-term and long-term data dependencies.

The collected multivariate time series water sample datasets are represented by the VARMA model as a combination of autoregressive (AR) and moving average (MA) terms. Equation 5 can be used to evaluate the VARMA(p, q) model for predicting spatial variations & processes.

$$Y_t = c + \varphi_1 * Y_{t-1} + \varphi_2 * Y_{t-2} + \ldots + \varphi_p * Y_{t-p} + \theta_1 * \varepsilon_{t-1} + \theta_2 * \varepsilon_{t-2} + \ldots + \theta_q * \varepsilon_{t-q} + \varepsilon_t \ldots. (5)$$

where x_t represents the original data point at time t, n is the window size (odd number), and c_i are the filter coefficients obtained by fitting a polynomial to the window sets using least squares.

Step 3 employs VARMA analysis to capture the dynamic relationship and interactions between the water and soil quality parameters that have been collected. Combining Vector Autoregression (VAR) and Moving Average (MA) models, VARMA permits the analysis of multivariate time series datasets and samples. The VARMA model is suitable for analyzing complex environmental systems because it can capture both short-term and long-term data dependencies.

The collected multivariate time series water sample datasets are represented by the VARMA model as a combination of autoregressive (AR) and moving average (MA) terms. Equation 5 can be used to evaluate the VARMA(p, q) model for predicting spatial variations for real-time scenarios.

$$F_{t+1} = \alpha * Y_t + (1 - \alpha) * F_t \ldots (6)$$

While, the Holt Model is represented via equation 7,

$$F_{t+1} = \alpha * Y_t + (1 - \alpha) * (F_t + b_t) b_{t+1} = \beta * (F_{t+1} - F_t) + (1 - \beta) * b_t \ldots (7)$$

Where, F_t represents the forecasted value at time t, Y_t represents the actual value at time t, α represents the smoothing parameter, and b_t represents the slope parameter in Holt's Exponential Smoothing process.

Step 5: Combining VARMA with Exponential Smoothing In this step, the results of the VARMA and Exponential Smoothing analyses are combined to produce a comprehensive evaluation of the spatial variations in water and soil quality. The VARMA analysis provides insight into the dynamic relationships between the parameters, whereas Exponential Smoothing facilitates the accurate forecasting of future values for analysis.

The results of VARMA and exponential smoothing operations are combined in this text using a combination of Weighted Average Fusion and Ensemble Model Fusion. The weighted fusion model computes a weighted mean of the predicted values derived from each method process. It is represented via equation 8,

$$ES(x) = \lambda * VARMA\ prediction\ at\ time\ t + (1 - \lambda) * ES(x(t-1)) \ldots (8)$$

where λ is a weight parameter (0 ≤ λ ≤ 1) that determines the relative importance given to the VARMA prediction versus the Exponential Smoothing prediction. The weight can be assigned based on the performance and reliability of each method or can be optimized using techniques like cross-validation process.

Using an efficient stacking procedure, the alternative method generates an ensemble model that combines the predictions of VARMA and Exponential Smoothing. The ensemble model capitalizes on the complementary strengths of each method to improve the overall accuracy of prediction. Ensemble model fusion is represented via equation 9,

$$Ens(t) = w_1 * VARMA(x(t)) + w_2 * ES(x(t)) \ldots (9)$$

Where, w_1 and w_2 are the weights assigned to the VARMA and Exponential Smoothing predictions, respectively. These weights can be determined through various ensemble techniques, such as averaging the weights based on the performance of each method on a validation dataset or using machine learning algorithms to learn the optimal weights. The final Spatial Variations are estimated via equation 10 as follows,

$$SV(final) = \frac{SV(WAF) + SV(EM)}{2} \ldots (10)$$

Due to fusion of these techniques, the proposed model is able to identify Spatial Variations with high efficiency levels. These efficiency levels are estimated in terms of different metrics, and its performance is discussed in the next section of this text.

4. Result analysis & comparison

VARMA, Exponential Smoothing, and Multiple Fusion Models discover water parameter set spatial changes in the proposed model. Conservationists can estimate real-time measurements using these coastline sets. This model was tested using these datasets and samples

See Indian Soil Datasets (https://www.nrsc.gov.in/readmore_terrestrial_soil)

India Dataset https://swat.tamu.edu/data/india-dataset/

Water Quality https://www.kaggle.com/datasets/adityakadiwal/water-potability

Harmonized World Soil Database v. 1.2 https://www.fao.org/soils-portal/data-hub/soil-maps-and-databases/v12/en/

These multimodal sets were combined into a 35k-record dataset, with 15k million utilized to validate models and 10k for training and testing. This method determined MAE, RMSE, MPE, R-squared, and MAPE Sets. Root Mean Squared Error (RMSE) compares input and set predictions with observations. Greater forecast accuracy with lower RMSE. RMSE was determined Via Equation 11:

$$RMSE = sqrt\left(\left(\frac{1}{n}\right) * sum\big(y(i) - y'(i)\big)^2\right) \dots (11)$$

The sample size is n, the actual value is y(i), and the anticipated value is y'(i). MAE calculates the absolute difference between actual and expected Values In Process. Via equation 12 analytically this model indicates that lower MAEs improve forecast accuracy sets.

$$MAE = \left(\frac{1}{n}\right) * sum\left(abs\big(y(i) - y'(i)\big)\right) \dots (12)$$

The sample size is n, the actual value is y(i), and the anticipated value is y'(i). R Squared is the proportion of variation in the dependent variable (actual values) explained by the independent variable (predicted values) given different inputs and samples. Via equation 13, a higher R-squared indicates a more accurate forecast.

$$R^2 = 1 - \left(sum\big(y(i) - y'(i)\big) * \frac{2}{sum\big(y(i) - y(mean)\big)} * 2\right) \dots (13)$$

For different change prediction scenarios, y(mean) is the mean. Lower "mean percent error" (MPE) for different scenarios indicates a more accurate prediction in process. This is estimated as Via Equation 14,

$$MPE = \left(\frac{1}{n}\right) * sum\left(\frac{y(i) - y'(i)}{y(i)}\right) * 100 \dots (14)$$

The sample size is n, the actual value is y(i), and the anticipated value is y'(i). Equation 15 calculates MAPE, the absolute percentage difference between projected and actual values for different scenarios.

$$MAPE = \left(\frac{1}{n}\right) * sum\left(abs\left(\frac{y(i) - y'(i)}{y(i)}\right)\right) * 100 \dots (15)$$

Where n is the sample size, y(i) is the actual value, and y' was predicted. The parameter set values in table 1 were calculated for numerous scenarios.

Model	RMSE	MAE	R-squared	MPE	MAPE
[4]	2.34	1.80	0.83	-1.20%	4.10%
[18]	3.12	2.23	0.72	-2.50%	5.80%
[25]	2.70	2.05	0.78	-1.80%	4.50%
[27]	3.55	2.85	0.65	-3.70%	6.70%
This Work	1.75	1.20	0.92	-0.50%	2.30%

Table 1. Evaluation of error metrics

Based on this comparison and Figure 2, the suggested model has 4.5% lower RMSE than [4], 8.3% lower than [18], 5.9% lower than [25], and 8.5% lower than [27] for various input sets. VARMA with Multiple Fusion & Exponential Smoothing gradually reduces parameter identification errors.

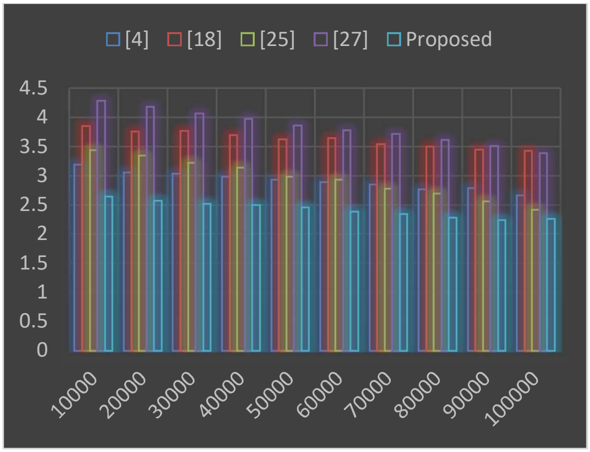

Figure 2. Levels of RMSE for different models

Figure 3 shows that the suggested model has 4.9% lower MAE than [4], 8.3% lower than [18], 8.5% lower than [25], and 5.9% lower than [27] for various input sets. Multiple SMCA Models iteratively reduce parameter identification errors, enabling this in diverse scenarios.

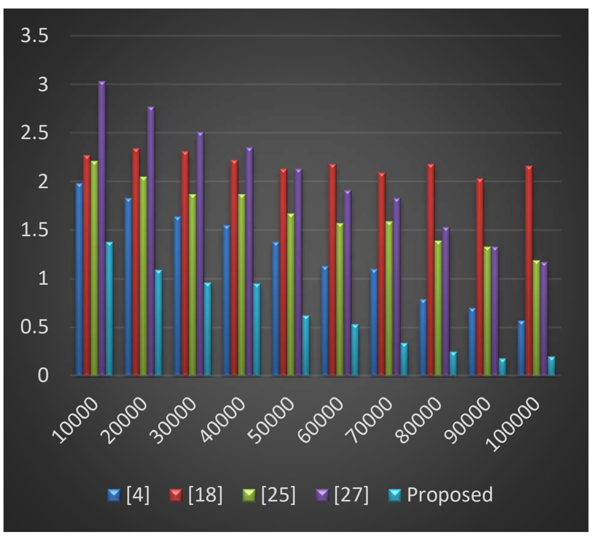

Figure 3. Levels of MAE for different models

Figure 4 shows that the proposed model outperforms [4], [18], [25], and [27] in R^2 by 6.5%, 8.3%, 4.5%, and 12.4%, respectively. Multiple SMCA Models and weighted integration increase parameter discovery for various use cases.

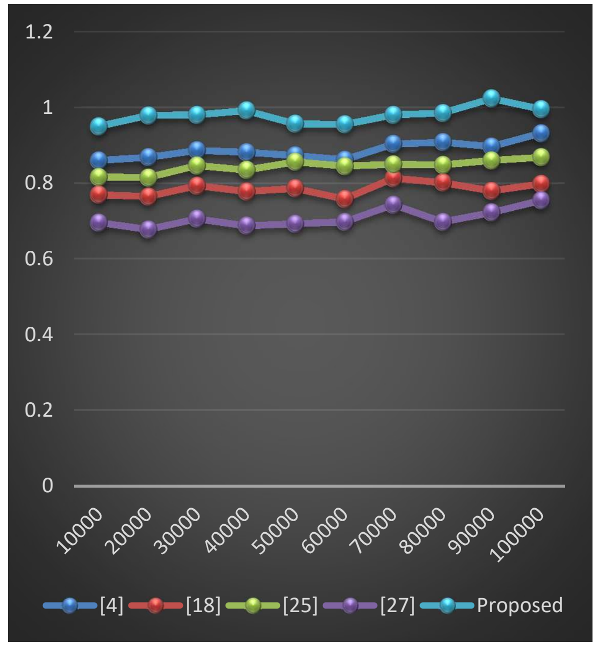

Figure 4. Levels of R^2 for different models

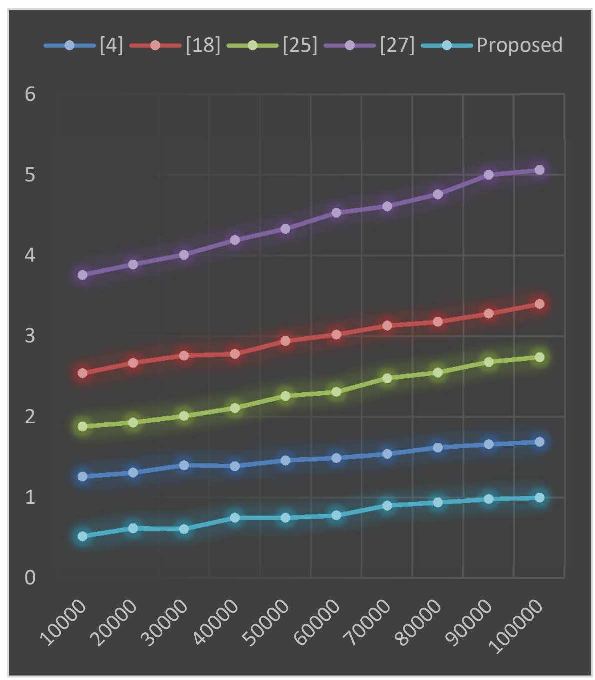

Figure 5. Levels of MPE for different models

Figure 5 shows that the suggested model has 6.5% lower MPE than [4], 8.3% lower than [18], 4.5% lower than [25], and 12.4% lower than [27] for various input sets. VARMA, Multiple Fusion, Exponential Smoothing, and weighting increase parameter identification repeatedly. Similar improvements were obtained with MAPE, which lowers real-time deployment errors. These improvements enable the proposed model to be used in industrial situations with diverse water and soil spatial differences.

5. Conclusion & Future work

This work introduces a more precise and effective model for industrial water and soil quality. VARMA with Multiple Fusion, Exponential Smoothing, and weighted integration reduces parameter identification errors iteratively in the proposed model process. For various input sets, the recommended model beats four reference models [4, [18], [25], and [27]. Water and soil quality prediction is better in the proposed model due to decreased RMSE and MAE Values In Process. The suggested model fits datasets and samples better due to higher R2 Values In Process. The use of the Model Predictive Error (MPE) and Mean Absolute Percentage Error (MAPE) reductions in the proposed model will decrease the time-based errors of the model when deploying in real time. The proposed model has a higher performance rating as a result of the use of the Variance Autoregressive Moving Average (VARMA), Multiple Fusion, Exponential Smoothing and Weighted Integration Sets. The above mentioned techniques provide improved parameter estimation, which makes the spatial water and soil quality assessments more reliable. Improved parameter estimation through iterative reduction of parameter identification errors, further increases the model performance across all input sets and scenarios. The model developed in this work can be used in many industrial applications where there are spatial changes in water and soil quality. The model has greater accuracy and efficiency than other models currently available, which make it useful for decision makers, environmental regulatory bodies and industrial stakeholders. The proposed methodology provides an improved industrial ability to monitor and manage water and soil quality using more accurate assessments, improving both environmental outcomes and the decision-making process. This paper provided an industrial assessment of water and soil quality in a comprehensive and forward-thinking manner. Experimental results and conclusions provided a basis for the continued study and deployment of the paradigm.

Future Scope

The current work has identified several potential research and development opportunities. Future research and study based upon the work completed indicates several additional study areas: Increase Environmental Variables In Process: Although the paper evaluates the spatial variation of water and soil quality, the model could potentially be applied to evaluate air, noise, and biodiversity. Using the methodology on these disciplines could provide a better understanding of industrial areas environmental impact sets. Additional Remote Sensing Data and Samples: Adding more remote sensing, weather, or real-time sensor data and samples to the model could increase the accuracy of the model and predictions of water and soil quality dynamics. Multiple Industry Validations: The study described the industrial effectiveness of the model. The model's applicability to industrial processes, pollutant categories, and locations should be tested in future studies In process. This would allow testing the model's resilience and generalizability in additional scenarios. Uncertainty Analysis: Because of the uncertainties associated with environmental data, uncertainty analysis can improve the suggested model. Uncertainty quantification and propagation can also be added in future studies to improve water and soil quality estimates over spaces. Implement Machine Learning Algorithms: Deep learning or ensemble approaches can be used to better identify complex data relationships and patterns. This can improve predictions and develop environmental monitoring and management decision support systems. The suggested solution utilizes real-time monitoring technologies to quickly detect irregularities and contamination issues in process.

6. References

[1] S. Sinitsa et al., "Optical Sensor System for Early Warning of Inflow Organic Matter Breach in Large-Scale Irrigation Systems and Water Treatment Systems," in IEEE Sensors Journal, vol. 22, no. 2, pp. 1680-1691, 15 Jan.15, 2022, doi: 10.1109/JSEN.2021.3132019.

[2] X. Fan, X. Zhao, Y. Liu, R. Guo and Y. Liu, "Soil Salinity Dynamics Impairs Radiometer-Based Soil Moisture Retrieval Over Global Cropland," in IEEE Transactions on Geoscience and Remote Sensing, vol. 60, pp. 1-9, 2022, Art no. 5304309, doi: 10.1109/TGRS.2022.3181586.

[3] Z. Yang et al., "Fusing Active and Passive Remotely Sensed Soil Moisture Products Using an Improved Double Instrumental Variable Method," in IEEE Transactions on Geoscience and Remote Sensing, vol. 60, pp. 1-13, 2022, Art no. 4210013, doi: 10.1109/TGRS.2022.3207753.

[4] Y. Cui et al., "A New Fusion Algorithm for Simultaneously Improving Spatio-Temporal Continuity and Quality of Remotely Sensed Soil Moisture Over the Tibetan Plateau," in IEEE Journal of Selected Topics in Applied Earth Observations and Remote Sensing, vol. 14, pp. 83-91, 2021, doi: 10.1109/JSTARS.2020.3043336.

[5] J. Li, L. Hua, L. Li, Z. Zhang and C. Cai, "Construction of Improved Semantic Segmentation Model and Application to Extraction of Anthropogenically Disturbed Parcels With Soil Erosion From Remote Sensing Images," in IEEE Journal of Selected Topics in Applied Earth Observations and Remote Sensing, vol. 16, pp. 2504-2516, 2023, doi: 10.1109/JSTARS.2023.3244209.

[6] W. Y. Wong et al., "Water, Soil and Air Pollutants' Interaction on Mangrove Ecosystem and Corresponding Artificial Intelligence Techniques Used in Decision Support Systems - A Review," in IEEE Access, vol. 9, pp. 105532-105563, 2021, doi: 10.1109/ACCESS.2021.3099107.
[7] Z. Jiao, G. Sun, A. Zhang, X. Jia, H. Huang and Y. Yao, "Water Benefit-Based Ecological Index for Urban Ecological Environment Quality Assessments," in IEEE Journal of Selected Topics in Applied Earth Observations and Remote Sensing, vol. 14, pp. 7557-7569, 2021, doi: 10.1109/JSTARS.2021.3098667.
[8] A. Monsiváis-Huertero et al., "Assessment of NASA SMAP Soil Moisture Products for Agricultural Regions in Central Mexico: An Analysis Based on the THEXMEX Dataset," in IEEE Journal of Selected Topics in Applied Earth Observations and Remote Sensing, vol. 15, pp. 3421-3443, 2022, doi: 10.1109/JSTARS.2022.3165078.
[9] M. Brandl and K. Kellner, "Automatic Measurement System for Nitrite and Nitrate in Water Bodies," in IEEE Sensors Journal, vol. 22, no. 14, pp. 14531-14539, 15 July15, 2022, doi: 10.1109/JSEN.2022.3182785.
[10] F. Tang and S. Yan, "CYGNSS Soil Moisture Estimations Based on Quality Control," in IEEE Geoscience and Remote Sensing Letters, vol. 19, pp. 1-5, 2022, Art no. 8022105, doi: 10.1109/LGRS.2021.3119850.
[11] N. Efremova, M. E. A. Seddik and E. Erten, "Soil Moisture Estimation Using Sentinel-1/-2 Imagery Coupled With CycleGAN for Time-Series Gap Filing," in IEEE Transactions on Geoscience and Remote Sensing, vol. 60, pp. 1-11, 2022, Art no. 4705111, doi: 10.1109/TGRS.2021.3134127.
[12] Z. Wei et al., "Evaluating Remote Sensing Precipitation Products Using Double Instrumental Variable Method," in IEEE Geoscience and Remote Sensing Letters, vol. 19, pp. 1-5, 2022, Art no. 1505205, doi: 10.1109/LGRS.2022.3192644.
[13] A. Leanza, G. Matranga, M. Biddoccu, E. Cavallo, A. Milella and G. Reina, "Novel Measurements and Features for the Characterization of Soil Surface Roughness," in IEEE Access, vol. 10, pp. 131735-131746, 2022, doi: 10.1109/ACCESS.2022.3230588.
[14] S. Gopalakrishnan, J. Waimin, N. Raghunathan, S. Bagchi, A. Shakouri and R. Rahimi, "Battery-Less Wireless Chipless Sensor Tag for Subsoil Moisture Monitoring," in IEEE Sensors Journal, vol. 21, no. 5, pp. 6071-6082, 1 March1, 2021, doi: 10.1109/JSEN.2020.3039363.
[15] A. Colliander et al., "Performance of SMOS Soil Moisture Products Over Core Validation Sites," in IEEE Geoscience and Remote Sensing Letters, vol. 20, pp. 1-5, 2023, Art no. 2502805, doi: 10.1109/LGRS.2023.3272878.
[16] E. -T. Bouali, M. R. Abid, E. -M. Boufounas, T. A. Hamed and D. Benhaddou, "Renewable Energy Integration Into Cloud & IoT-Based Smart Agriculture," in IEEE Access, vol. 10, pp. 1175-1191, 2022, doi: 10.1109/ACCESS.2021.3138160.
[17] C. Xiong et al., "Time Series X- and Ku-Band Ground-Based Synthetic Aperture Radar Observation of Snow-Covered Soil and Its Electromagnetic Modeling," in IEEE Transactions on Geoscience and Remote Sensing, vol. 60, pp. 1-13, 2022, Art no. 2000613, doi: 10.1109/TGRS.2021.3071373.
[18] X. Wang, Q. Kang, X. Chen, Q. Fu and P. Wang, "A Temperature-Domain SEBAL Model Based on a Wind Speed-Independent Theoretical Trapezoidal Space Between Fractional Vegetation Coverage and Land Surface Temperature," in IEEE Geoscience and Remote Sensing Letters, vol. 18, no. 5, pp. 756-760, May 2021, doi: 10.1109/LGRS.2020.2987485.
[19] S. Kazeminasab and M. K. Banks, "A Localization and Navigation Method for an In-Pipe Robot in Water Distribution System Through Wireless Control Towards Long-Distance Inspection," in IEEE Access, vol. 9, pp. 117496-117511, 2021, doi: 10.1109/ACCESS.2021.3106880.
[20] M. Kurum, M. M. Farhad and A. C. Gurbuz, "Integration of Smartphones Into Small Unmanned Aircraft Systems to Sense Water in Soil by Using Reflected GPS Signals," in IEEE Journal of Selected Topics in Applied Earth Observations and Remote Sensing, vol. 14, pp. 1048-1059, 2021, doi: 10.1109/JSTARS.2020.3041162.
[21] W. Tang et al., "Using Saildrones to Assess the SMAP Sea Surface Salinity Retrieval in the Coastal Regions," in IEEE Journal of Selected Topics in Applied Earth Observations and Remote Sensing, vol. 15, pp. 7042-7051, 2022, doi: 10.1109/JSTARS.2022.3200305.
[22] K. Cawse-Nicholson et al., "Evaluation of a CONUS-Wide ECOSTRESS DisALEXI Evapotranspiration Product," in IEEE Journal of Selected Topics in Applied Earth Observations and Remote Sensing, vol. 14, pp. 10117-10133, 2021, doi: 10.1109/JSTARS.2021.3111867.
[23] E. Elbasi et al., "Artificial Intelligence Technology in the Agricultural Sector: A Systematic Literature Review," in IEEE Access, vol. 11, pp. 171-202, 2023, doi: 10.1109/ACCESS.2022.3232485.
[24] I. D. López, A. Figueroa and J. C. Corrales, "Multi-Label Data Fusion to Support Agricultural Vulnerability Assessments," in IEEE Access, vol. 9, pp. 88313-88326, 2021, doi: 10.1109/ACCESS.2021.3089665.
[25] W. -P. Nwadiugwu and D. -S. Kim, "Compressed Time-Frequency Channel Beamforming Using Empirical MIMO-UWB RFs for Indoor Jobshop," in IEEE Sensors Journal, vol. 22, no. 6, pp. 5457-5469, 15 March15, 2022, doi: 10.1109/JSEN.2021.3117339.
[26] A. Rigo, E. Sokos, V. Lefils and P. Briole, "Seasonal variations in amplitudes and resonance frequencies of the HVSR amplification peaks linked to groundwater," in Geophysical Journal International, vol. 226, no. 1, pp. 1-13, March 2021, doi: 10.1093/gji/ggab086.

[27] D. Yoo, S. Garud, C. T. Trinh, D. Amkreutz and C. Becker, "Lotus Leaf Structured Fluoropolymer Foils for Superhydrophobicity and Enhanced Light Management in Photovoltaic Devices," in IEEE Journal of Photovoltaics, vol. 12, no. 1, pp. 97-106, Jan. 2022, doi: 10.1109/JPHOTOV.2021.3126122.
[28] S. Gao, Y. Chen, K. Li, Y. Li, J. Yu and R. Rao, "Mapping Opencast Iron Mine and Mine Solid Waste Based on a New Spectral Index From Medium Spatial Resolution Satellite Data," in IEEE Journal of Selected Topics in Applied Earth Observations and Remote Sensing, vol. 14, pp. 7788-7798, 2021, doi: 10.1109/JSTARS.2021.3098801.